Effect of Lithium on Physical and Sensing Properties of Titanium Oxide Nanostructured Thin Films Prepared by Chemical Spray Pyrolysis

Ahmed Naji Al-Jamal[1] , Oday Ali Chichan[2], Hanaa Kadem Essa[3], Shaymaa A. Hussein[4], Hadi Ahmed Hussin[3], Sami Salman Chiad[3], Nadir Fadhil Habubi[3,5,6] and Yassin Hasan Kadhim[7]
[1]*Department of Biomedical Engineering, College of Engineering, University of Babylon, 51001 Hillah, Babylon, Iraq*
[2]*Department of Physics, College of Education for Pure Sciences, University of Babylon, 51001 Hillah, Babil, Iraq*
[3]*Department of Physics, College of Education, Mustansiriyah University, 10052 Baghdad, Iraq*
[4]*Department of Medical Laboratory Techniques, Al-Manara College for Medical Science, 62001 Al-Amarah, Iraq*
[5]*Department of Radiation and Sonar Technologies, Alnukhba University College, 10013 Baghdad, Iraq*
[6]*Department of Radiology Techniques, Al-Qalam University College, 36001 Kirkuk, Iraq*
[7]*Department of Optics Techniques, College of Health and Medical Techniques, AL-Mustaqbal University, 51001 Hillah, Babylon, Iraq*
pure.oday.ali@uobabylon.edu.iq, dr.sami@uomustansiriyah.edu.iq

Keywords: Li-Doped TiO2 Thin Films, Structural, Morphological Optical, Chemical Spray Pyrolysis.

Abstract: Li-doped titanium oxide thin films are grown through Spray Pyrolysis (SP) method. XRD peaks showed that samples were polycrystalline. The appropriate peak was at (121) equivalent to $2\theta = 30.70^{\circ}$, the Grain size (D) increased from 9.58 nm to 10.17 nm, whereas strain (ε) decreased from 36.17 to 34.08, whilst dislocation density (δ) decreased from 108.96 to 96.68. According to the AFM photo, surface roughness declined (8.08 - 3.67) nm when TiO_2 was increased to 4% Li. The average particle size values were 88.78, 85.62, and 60.89 nm for TiO2, TiO_{2}:2 % Li, and TiO_2:4% Li, respectively. The transmittance of TiO_2 and TiO_2: Li films reduced from 85 TiO_2 % to 75 % as Lithium content rise from 1 to 4 at%. Research indicates that the absorption coefficient reduces as the lithium content rises, whereas the bandgap energy, extinction coefficient, and refractive index decline as the lithium content rises. The TiO_2 gas sensor showed increased resistance at 200 ppm NH3, with 4% Li doping having the highest. Higher Li doping in TiO_2 decreases sensor sensitivity to NH3 gas, with a reduction at all concentrations.

1 INTRODUCTION

Due to its numerous advantageous attributes, titanium oxide (TiO_2) is an intriguing substance that has the potential to be employed in numerous applications. These properties are high transparency, non-toxicity, high refractive index, affordability, good optical and electrical properties, and chemical stability [1]. In addition, TiO_2 can be deposited on large areas and is inexpensive, making it an appropriate material for industrial use. Due to the preferred properties, TiO_2 is utilized in multiple uses, including optoelectronics devices, gas sensors, photocatalyst photoelectrochemical water splitting, and solar energy conversion. [2]-[4]. Numerous techniques are employed to deposit TiO_2 thin films, including e-beam evaporation [5], sol-gel [6], sputtering [7], precipitation [9], anodic oxidation [9], hydrothermal [10], PLD[11], CVD [12] and CSP [13]. However, the spray pyrolysis deposition method has appropriate advantages: affordable deposition equipment, the ability to coat large areas, and controlling the composition is easy [14]. The Chemical Spray Pyrolysis technique fabricated the Undoped TiO_2 and TiO_2: Li thin films to get inexpensive large-area films with good characteristics. The article discusses the alteration in physical characteristics of TiO_2 thin films as a result of Li doping.

2 EXPERIMENTAL

Thin films of TiO_2 and TiO_2: Li grown by CSP technique. The base was cleaned with chromic acid for 4 hours, rinsed with running water for 20 minutes, and in an ultrasonic bath filled with absolute ethanol for 8 minutes. 0.1M of $TiCl_2.2H_2O$ was supplied from Sigma-Aldrich Chemicals, with 0.1M of $LiCl_2.4H_2O$ from Merck Chemicals. Various Li contents were used (0, 2, 4%). The following were the deposition conditions: the base temperature was 400 degrees Celsius, The separation between the substrate and the outlet was 28 cm, the spraying rate was 10s, stopping by 90 s to avoid cooling, spray rate was 5 ml per second, and N_2 is being used as the gas transport. Film thickness was measured employing weighing method, and it was discovered to be 300±30 nm. XRD investigated the structural properties. AFM is used to probe sample surface. A double beam spectrophotometer was utilized to obtain transmittance of the entended samples. Gas sensitivity was measured by change in resistance.

3 RESULTS AND DISCUSSIONS

Figure 1 represents XRD peaks of all fabricated thin films of Undoped TiO_2, doped with Li content of 0.0, 2.0% and 4.0%. From Figure 1, the peaks of TiO_2 and TiO_2: Li thin film is located at 25.34°, 30.72°, 49.13° and 64.12° that belong to (111), (121), (132) and (203) planes respectively. A high peak at (121) is fit with ICDD card no 29-1360 [14], [15].

Grain size (D) was evaluated via (1) [16]:

$$D = \frac{k\,\lambda}{\beta cos\theta}. \quad (1)$$

Where k = 0.9, λ =1.54 Å, θ is Bragg's angle, and β is FWHM. Table 1 provides the obtained data. D rose from 9.58 nm to 10.17 nm, according to Lithium content, as presented in Table 1.
The δ was established by [17], [18]:

$$\delta = \frac{1}{D^2}. \quad (2)$$

Table 1. displays δ decreased from 10.96 to 96.68 with Lithium content.

Similarly, the lattice strain ε was determined according to [19]:

$$\varepsilon = \frac{\beta cos\theta}{4}. \quad (3)$$

It is seen that ε dropped from 36.17 to 34.08 with Lithium concentration (Table 1). Structural parameters (S_P) are seen in Figure 2.

AFM micrographs are shown in Figure 3. The domain showed tightly packed columnar crystals with sharp peaks. As TiO_2:4% Li increases, surface roughness (R_a) declined (8.08 - 3.67) nm. From Figure 3, the average Particle size (P_{Av}) and rms values were (88.78, 85.62 and 60.89) nm and 9.23, 8.12 and 3.89) nm for Undoped TiO_2, TiO_2: 2% Li and TiO_2: 4% Li respectively [20]-[23]. Table 2 displays AFM parameters P_{AFM}

Table 1: Structural parameters of D, Eg and SP of deposit films.

Specimen	2 θ (°)	(hkl) Plane	FWHM (°)	E_g eV	D nm	δ(× 10^{14}) lines/m^2	ε (× 10^{-4})
TiO_2 Undoped	30.72	121	0.85	3.28	9.58	108.96	36.17
TiO_2: 2% Li	30.70	121	0.84	3.22	9.81	103.91	35.34
TiO_2: 4% LI	30.65	121	0.81	3.17	10.17	96.68	34.08

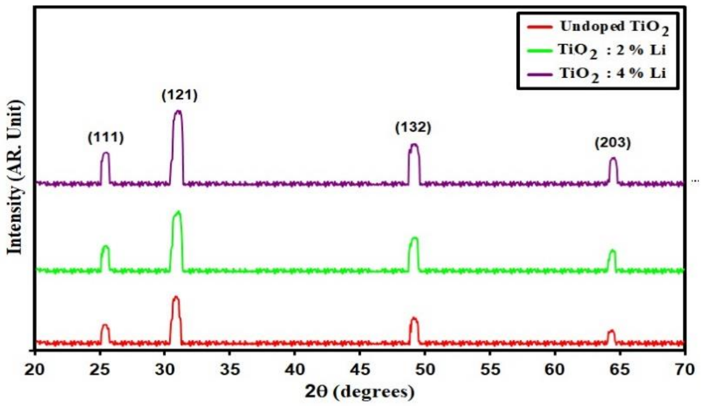

Figure 1: XRD styles of entended films.

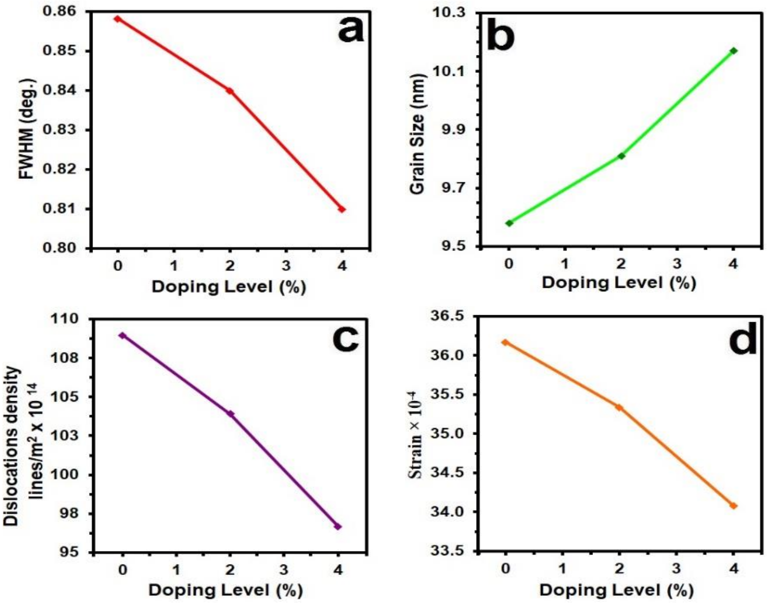

Figure 2: SP of the deposit films.

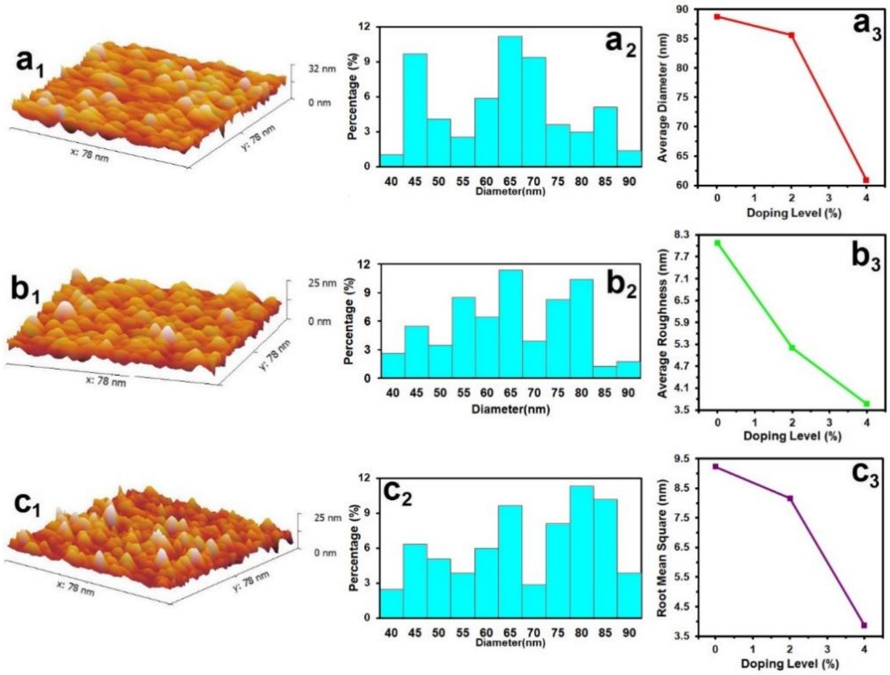

Figure 3: AFM images, granularly distributed and diversity of PAFM.

Table 2: PAFM of the deposit films.

Samples	P_{AV} nm	R_a nm	rms nm
Undoped TiO_2	88.78	8.08	9.23
TiO_2: 1% Sn	85.62	5.20	8.12
TiO_2: 3% Sn	60.89	3.67	3.89

The spectral distribution of transmittance (T) is offered in Figure 4. From Figure 4, it is possible to see declines in T as Lithium content increases [24]-[26].

The optical absorption coefficient (α) was evaluated via the following (4) [27]:

$$\alpha = \frac{2.303A}{t}. \quad (4)$$

The α was presented in Figure 5, and α values were rise by increasing Li content [28], [29].

Using Tauc's relation, bandgap E_g was found from (5) [30]:

$$(\alpha h\nu) = A\left(h\nu - E_g\right)^{\frac{1}{2}}. \quad (5)$$

From Figure 6 the bandgap is calculated from $(\alpha h\upsilon)^2$ versus hυ representing E_g declined from 3.28 eV to 3.17 eV with irising lithium content [31]-[33].

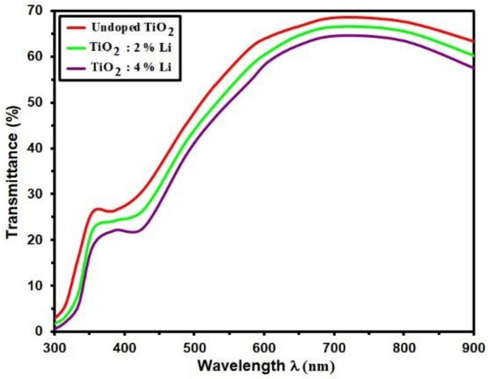

Figure 4: Transmittance (T) of the deposit films.

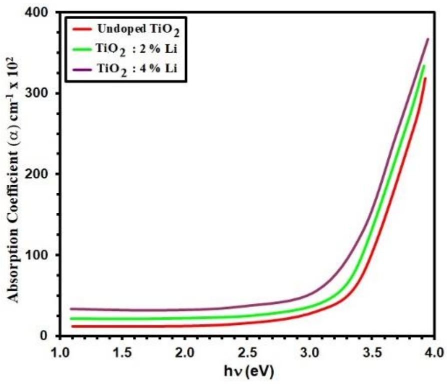

Figure 5: Absorption coefficient (α) of grown films.

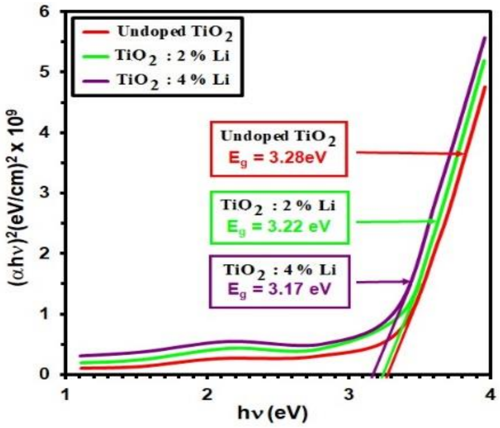

Figure 6: Plot of $(\alpha h\nu)^2$ versus hν for the TiO2 with different Li doping.

Extinction coefficient (k) is evaluated via (6) [34], [35]:

$$k = \frac{\alpha\lambda}{4\pi}. \quad (6)$$

The λ is the wavelength, Figure 7 offers k via λ , showing that k decreases with increasing Lithium concentration.

Refractive index (n) was evaluated as [36], [37]:

$$n = \left(\frac{1+R}{1-R}\right) + \sqrt{\frac{4R}{(1-R)^2} - k^2}. \quad (7)$$

R is reflectance Figure 8 offers the relationship between n and λ. From this Figure 8, it's clear that n decreases with the rise of Lithium content [38]-[40].

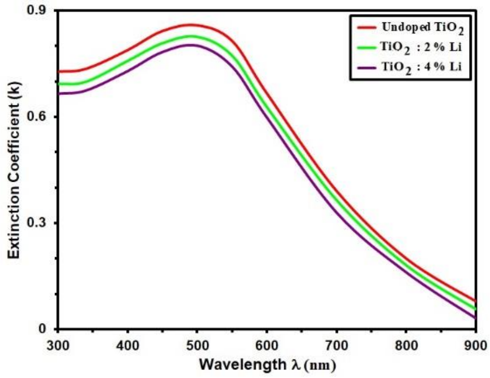

Figure 7: Extinction coefficient (k) of the deposit films.

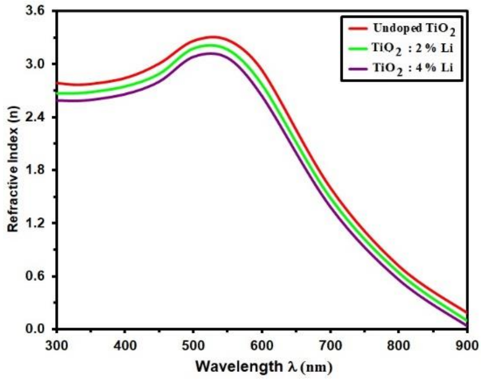

Figure 8: Refractive index (n) of entended films.

The sensitivity (s), is determined using the (8). below [41], [42]:

$$Sensitivity = \frac{\Delta R}{R_g} = \left|\frac{R_g - R_a}{R_g}\right| \times 100\ \% \qquad (8)$$

The gas sensor, was tested with 200 ppm NH_3. Figure 9 shows resistance-time data for TiO_2 and Li-doped TiO_2 at 125°C. NH_3 exposure causes oxidation, releasing electrons from O_2^+ ions to CB rising resistance and potential barrier [49]-[51]. The TiO_2 film with 4% Li showed the highest resistance, enhancing the material's sensing response [52]-[54].

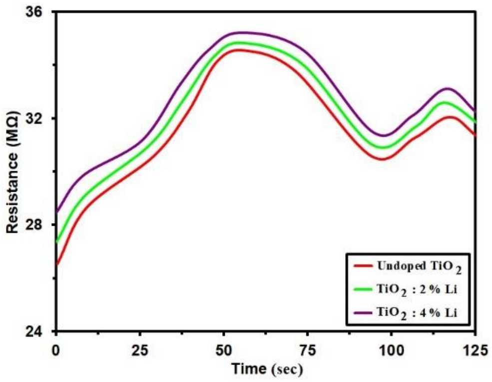

Figure 9: Resistance as a function of operating time for Undoped and TiO2: Li films.

Figure 10 illustrates that sensitivity to NH_3 decreases with increasing Li doping in TiO_2 films due to charge carrier recombination, with TiO_2: 4% Li showing the lowest sensitivity [55-58]. For different doping levelsundoped TiO_2, TiO_2: 2% Li, and TiO_2: 4% Li sensitivity decreased from 21,7 % to 4.1 % at 100 ppm, from 24.4 % to 7.9 % at 150 ppm, and from 28.7 % to 9.3 % at 200 ppm [59-60]. The reduction in sensitivity for undoped TiO_2, TiO_2: 2% Li, and TiO_2: 4% Li indicates that higher Li doping levels result in decreased sensor responsiveness to NH_3 gas [61], [62].

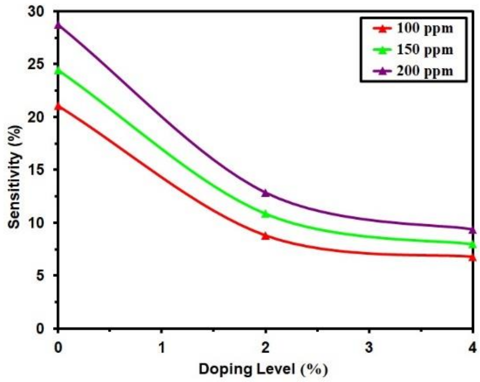

Figure 10: Sensitivity of Undoped and TiO2: Li films with different dopant.

4 CONCLUSIONS

The influence of two Lithium contents (2% and 4%) on Undoped Titanium Oxide films were studied. Lithium doped Titanium Oxide films were The entended films are grown by CSP. X-ray diffraction results confirmed the polycrystalline nature of the films, with the dominant peak observed at the (121) plane. As the Li content increased, the grain size increased slightly while both dislocation density and lattice strain decreased. AFM analysis revealed that surface roughness and average particle size decreased with higher Li doping, suggesting a smoother, more compact surface. Optically, increased Li content led to a reduction in transmittance, extinction coefficient, refractive index, and bandgap energy (from 3.28 eV to 3.17 eV), while the absorption coefficient increased. In terms of gas sensing behavior, all samples demonstrated a p-type response to NH_3 gas at 125°C, with the undoped TiO_2 showing the highest sensitivity. However, as the Li concentration increased, the sensitivity to NH_3 consistently decreased. These results suggest that while Li doping enhances structural and optical properties, it adversely affects gas sensing performance, indicating a trade-off between optical and sensing functionalities in doped TiO_2 films.

ACKNOWLEDGEMENTS

The authors appreciate the support of Mustansiriyah University.

REFERENCES

[1] G. Pecchi, P. Reyes, P. Sanhueza, and J. Villasenor, "Photocatalytic degradation of pentachlorophenol on TiO2 sol-gel catalysts," Chemosphere, vol. 43, p. 141, 2001.

[2] I. Oja, A. Mere, M. Krunks, R. Nisumaa, C. H. Solterbeck, and M. Es-Souni, "Structural and electrical characterization of TiO2 films grown by spray pyrolysis," Thin Solid Films, vol. 515, no. 2, pp. 674-677, 2006.

[3] N. R. Mathews, E. R. Morales, M. A. Cortés-Jacome, and J. A. Toledo Antonio, "TiO2 thin films - influence of annealing temperature on structural, optical and photocatalytic properties," Sol. Energy, vol. 83, no. 9, pp. 1499-1508, 2009.

[4] A. D. L. Andronic and S. Manolache, "TiO2 thin films prepared by spray pyrolysis deposition (SPD) and their photocatalytic activities," J. Optoelectron. Adv. Mater., vol. 9, pp. 1403-1406, 2007.

[5] Y. Leprince-Wang and K. Yu-Zhang, "Study of the growth morphology of TiO2 thin films by AFM and TEM," Surf. Coat. Technol., vol. 140, no. 2, pp. 155-160, 2001.

[6] V. Manole, M. Dobromir, M. G., R. Mallet, G. Rusu, and D. Luca, "Optical properties of Nb-doped TiO2 thin films prepared by sol-gel method," vol. 39, no. 4, pp. 4771-4776, 2013.

[7] C. Zhang, W. Ding, H. Wang, W. Chai, and D. Ju, "Influences of working pressure on properties of TiO2 films deposited by DC pulse magnetron sputtering," J. Environ. Sci., vol. 21, no. 6, pp. 741-744, 2009.

[8] F. C. Chung, Z. Zhu, P. Y. Luo, R. J. Wu, and W. Li, "Fabrication of a Au@SnO core-shell structure for gaseous formaldehyde sensing at room temperature," Sensors Actuat. B: Chem., vol. 199, pp. 314-319, 2014.

[9] L. Lu-Lin, T. Chiau-Yiag, and W. Hui-Ping, "Morphologic characterization of anodic titania nanotube arrays for dye-sensitized solar cells," J. Chinese Chem. Soc., vol. 57, no. 5B, pp. 1147-1150, 2010.

[10] X. F. Wu, H. Y. Song, J. M. Yoon, Y. T. Yu, and Y. F. Chen, "Synthesis of core-shell Au@TiO2 nanoparticles with truncated wedge-shaped morphology and their photocatalytic properties," Langmuir, vol. 25, no. 11, pp. 6438-6447, 2009.

[11] M. P. Moret, R. Zallen, D. P. Vijay, and S. B. Desu, "Brookite-rich titania films made by pulsed laser deposition," Thin Solid Films, vol. 366, pp. 10-12, 2000.

[12] D. Mardare, F. Iacomi, N. Cornei, M. Girtan, and D. Luca, "Undoped and Cr-doped TiO2 thin films obtained by spray pyrolysis," Thin Solid Films, vol. 518, no. 16, pp. 4586-4589, 2010.

[13] Z. Ding, X. Hu, P. L. Yue, G. Q. Lu, and P. F. Greenfield, "Synthesis of anatase TiO2 supported on porous solids by chemical vapor deposition," Catal. Today, vol. 68, p. 173, 2001.

[14] Z. Tan, K. Sato, and S. Ohara, "Synthesis of layered nanostructured TiO2 by hydrothermal method," Adv. Powder Technol., vol. 26, no. 1, pp. 296-302, 2015.

[15] Z. Tan, K. Sato, and S. Ohara, "Synthesis of layered nanostructured TiO2 by hydrothermal method," Adv. Powder Technol., vol. 26, no. 1, pp. 296-302, 2015.

[16] P. Kajitvichyanukul, J. Ananpattarachai, and S. Pongpom, "Sol-gel preparation and properties study of TiO2 thin film for photocatalytic reduction of chromium (VI) in photocatalysis process," Sci. Technol. Adv. Mater., vol. 6, p. 352, 2005.

[17] J. He, I. Ichinose, T. Kunitake, and A. Nakao, "In situ synthesis of noble metal nanoparticles in ultrathin TiO2-gel films by a combination of ion-exchange and reduction processes," Langmuir, vol. 18, no. 25, pp. 10005-10010, 2002.

[18] H. T. Salloom, E. H. Hadi, N. F. Habubi, S. S. Chiad, M. Jadan, and J. S. Addasi, "Characterization of silver content upon properties of nanostructured nickel oxide thin films," Digest J. Nanomater. Biostruct., vol. 15, no. 4, pp. 1189-1195, 2020.

[19] F. U. Khan, M. Zubair, I. Khan, M. Z. Ansar, M. K. Alamgir, and S. Nadeem, "Effect of annealing temperature on structural and optical properties of Cu-TiO2 thin film," Int. J. Tech. Res. Appl., spec. issue, vol. 37, no. 8, pp. 2320-8163, 2016.

[20] M. R. Behforooz and H. Kangarlou, "Structural and optical properties of TiO2/Ag/TiO2 multi layers," Appl. Sci. Res., vol. 2, no. 10, pp. 10234-10240, 2012.

[21] R. S. Ali, N. A. H. Al Aaraji, E. H. Hadi, K. H. Abass, N. F. Habubi, and S. S. Chiad, "Effect of lithium on structural and optical properties of nanostructured CuS thin films," J. Nanostructures, vol. 10, no. 4, pp. 810-816, 2020.

[22] P. Peerakiatkhajohn, W. Onreabroy, C. Chawengkijwanich, and S. Chiarakorn, "Preparation of visible-light-responsive TiO2 doped Ag thin film on PET plastic for BTEX treatment," vol. 2, pp. 121-125, 2011.

[23] A. P. Caricato, A. Luches, G. Leggieri, M. Martino, and R. Rella, "Matrix-assisted pulsed laser deposition of polymer and nanoparticle films," Vacuum, vol. 86, no. 6, pp. 661-666, 2012.

[24] L. Sun, J. Li, C. Wang, S. Li, Y. Lai, H. Chen, and C. Lin, "Ultrasound aided photochemical synthesis of Ag loaded TiO2 nanotube arrays to enhance photocatalytic activity," J. Hazard. Mater., vol. 171, no. 1-3, pp. 1045-1050, 2009.

[25] N. A. He, I. Ichinose, and T. Kunitake, "In situ synthesis of noble metal nanoparticles in ultrathin TiO2-gel films by a combination of ion-exchange and reduction processes," Langmuir, vol. 18, pp. 10005-10010, 2002.

[26] R. Mechiakh, N. Bensedrine, and R. Chtourou, "Sol-gel synthesis, characterization and optical properties of mercury-doped TiO2 thin films deposited on glass substrates," Appl. Surf. Sci., vol. 257, pp. 9103-9109, 2011.

[27] C. Manoharan and R. Sridhar, "Physical properties of spray pyrolysed TiO2 films," Int. J. Recent Sci. Res., vol. 3, pp. 775-777, 2012.

[28] K. Okimura, "Low temperature growth of rutile TiO2 films in modified RF magnetron sputtering," Surf. Coat. Technol., vol. 135, pp. 286-290, 2001.

[29] R. S. Ali, M. K. Mohammed, A. A. Khadayeir, Z. M. Abood, N. F. Habubi, and S. S. Chiad, "Structural and optical characterization of sprayed nanostructured indium doped Fe2O3 thin films," J. Phys.: Conf. Ser., vol. 1664, no. 1, 012016, 2020.

[30] J.-Y. Lee, W. Y. Lee, D.-K. Choi, and J. Oh, "Structure and properties of Co-doped TiO2 thin films on Si(100) by pulsed laser deposition method," J. Ceramic Processing Res., vol. 7, no. 1, pp. 58-61, 2006.

[31] M. Radoičić, Z. V. Šaponjić, M. T. Marinović, S. P. Cincović, B. N. Bibić, and J. M. Nedeljković, "The influence of shaped TiO2 nanofillers on the thermal properties of poly(vinyl alcohol)," J. Serbian Chem. Soc., vol. 76, pp. 1-23, 2011.

[32] A. A. Khadayeir, R. I. Jasim, S. H. Jumaah, N. F. Habubi, and S. S. Chiad, "Influence of substrate temperature on physical properties of nanostructured ZnS thin films," J. Phys.: Conf. Ser., vol. 1664, no. 1, 2020.

[33] M. Landmann, E. Rauls, and W. G. Schmidt, "The electronic structure and optical response of rutile, anatase and brookite TiO2," J. Phys.: Condens. Matter, vol. 24, p. 195503, 2012.

[34] C. Yang, H. Fan, Y. Xi, J. Chen, and Z. Li, "Effects of depositing temperatures on structure and optical properties of TiO2 film deposited by ion beam assisted electron beam evaporation," Appl. Surf. Sci., vol. 254, pp. 2685-2689, 2008.

[35] J. Y. Kim, D.-W. Kim, H. S. Jung, and K. S. Hong, "Influence of anatase-rutile phase transformation on dielectric properties of sol-gel derived TiO2 thin films," Jpn. J. Appl. Phys., vol. 44, pp. 6148-6151, 2005.

[36] S. S. Chiad, A. S. Alkelaby, and K. S. Sharba, "Optical conduct of nanostructure Co3O4 rich highly doping Co3O4:Zn alloys," J. Global Pharma Technol., vol. 11, no. 7, pp. 662-665, 2020.

[37] V. G. Besserguenev, R. J. F. Pereira, M. C. Mateus, I. V. Khmelinskii, R. C. Nicula, and E. Burkel, "TiO2 thin film synthesis from complex precursors by CVD, its physical and photocatalytic properties," Int. J. Photoenergy, vol. 5, pp. 99-105, 2003.

[38] W. Yang and C. A. Wolden, "Plasma-enhanced chemical vapor deposition of TiO2 thin films for dielectric applications," Thin Solid Films, vol. 515, pp. 1708-1713, 2006.

[39] S. S. Chiad, H. A. Noor, O. M. Abdulmunem, and N. F. Habubi, "Optical and structural properties of Ni-doped Co3O4 nanostructure thin films via CSPM," J. Phys.: Conf. Ser., vol. 1362, no. 1, 2019.

[40] B. M. Henry, "Method of depositing titanium dioxide (rutile) as a gate dielectric for MIS device fabrication," U.S. Patent 4,200,474, 1978.

[41] C. H. Heo, S.-B. Lee, and J.-H. Boo, "Deposition of TiO2 thin films using RF magnetron sputtering method and study of their surface characteristics," Thin Solid Films, vol. 475, pp. 183-188, 2005.

[42] H. Pulker, G. Paesold, and E. Ritter, "Refractive indices of TiO2 films produced by reactive evaporation of various titanium-oxygen phases," Appl. Opt., vol. 15, pp. 2986-2991, 1976.

[43] A. Sharma, A. Gouldstone, S. Sampath, and R. J. Gambino, "Anisotropic electrical conduction from heterogeneous oxidation states in plasma sprayed TiO2 coatings," J. Appl. Phys., vol. 100, p. 114906, 2006.

[44] H. P. Deshmukh, P. S. Shinde, and P. S. Patil, "Structural, optical and electrical characterization of spray-deposited TiO2 thin films," Mater. Sci. Eng. B, vol. 130, nos. 1-3, pp. 220-227, 2006.

[45] I. J. Panneerdoss, S. J. Jeyakumar, and M. Jothibas, "Characteristic comparison of TiO2 thin films with an inorganic and organic precursor at different molarities by spray pyrolysis," Int. J. Eng. Sci., vol. 4, no. 11, pp. 15-20, Nov. 2014.

[46] M. M. Hasan, A. S. M. A. Hasseeb, R. Saidur, and H. H. Masjuki, "Effect of annealing treatment on optical properties of anatase TiO2 thin films," Int. J. Chem. Biomol. Eng., vol. 1, pp. 93-97, 2008.

[47] B. Ravidhas, B. Anitha, A. Moses Ezhil Raj, and K. Ravichandran, "Effect of nitrogen-doped titanium dioxide (N-TiO2) thin films by jet nebulizer spray technique suitable for photoconductive study," J. Mater. Sci.: Mater. Electron., [Online]. Available: https://doi.org/10.1007/s10854-015-2871-0.

[48] C. T. Kim, "Photoelectric characteristics of nano TiO2 film prepared by spraying pyrolysis method," Int. J. Nano Stud. Technol., May 8, 2015.

[49] J. Millman, Microelectronics: Digital and Analog Circuits and Systems. New York: McGraw-Hill, 1979.

[50] W. W. Xu, R. Kershaw, K. Dwight, and A. Wold, "Preparation and characterization of TiO2 films by a novel spray pyrolysis method," Mater. Res. Bull., vol. 25, pp. 1385-1392, 1990.

[51] A. A. Yousif, K. A. Aadim, and N. A. Hamzah, "Influence of Ag doping on optical properties of nanocrystalline titanium dioxide prepared by PLD," IOSR J. Appl. Phys., vol. 8, no. 5, pp. 50-56, 2016.

[52] V. Sivaranjan, P. Deepa, and P. Philominathan, "Thin films of TiO2-MoO3 binary oxides obtained by an economically viable and simplified spray pyrolysis technique for gas sensing application," Int. J. Thin Film Sci. Technol., no. 2, pp. 125-131, 2015.

[53] M. R. Kozlowski, P. S. Tyler, W. H. Smyrl, and R. T. Atanassov, "Anodic TiO2 thin films photoelectrochemical, electrochemical, and structural study of heat-treated and RuO2-modified films," J. Electrochem. Soc., vol. 136, pp. 442-450, 1989.

[54] N. Inoue, H. Yuasa, and M. Okoshi, "TiO2 thin films prepared by PLD for photocatalytic applications," Appl. Surf. Sci., vols. 197-198, pp. 393-397, 2002.

[55] M. Thakurdesai, D. Kanjilal, and V. Bhattacharyya, "Effect of rapid thermal annealing on nanocrystalline TiO2 thin films synthesized by swift heavy ion irradiation," Appl. Surf. Sci., vol. 12, pp. 1-25, 2012.

[56] Y. Hou, D. Zhuang, G. Zhang, M. Zhao, and M. Wu, "Influence of annealing temperature on the properties of titanium oxide thin film," Appl. Surf. Sci., vol. 218, p. 98, 2003.

[57] M. Hasan, A. Haseeb, H. Masjuki, and R. Saidur, "Influence of substrate temperatures on structural, morphological and optical properties of RF sputtered anatase TiO2 films," Arab. J. Sci. Eng., vol. 35, pp. 147-156, 2010.

[58] M. M. Hasan, A. S. M. A. Hasseeb, R. Saidur, and H. H. Masjuki, "Effect of annealing treatment on

optical properties of anatase TiO2 thin films," Int. J. Chem. Biomol. Eng., vol. 1, pp. 93-97, 2008.

[59] Y. Kubota et al., "Application of titanium oxide in solar cell," J. Photochem., vol. 141, p. 215, 2001.

[60] A. R. Phani et al., "Structural characterization of iron titanium oxide synthesized by sol-gel spin coating technique," Mater. Lett., vol. 50, pp. 240-245, 2001.

[61] A. A. Hateef, "Studying the optical and electrical properties of TiO2 thin films prepared by chemical spray pyrolysis technique and their application in solar cells," M.Sc. thesis, Al-Mustansiriyah Univ., Coll. Sci., Dept. Phys., 2010.

[62] D. J. Won, C. H. Wang, H. K. Jang, and D. J. Choi, "Effects of thermally induced anatase-to-rutile phase transition in MOCVD-grown TiO2 films on structural and optical properties," Appl. Phys. A, vol. 73, no. 5, pp. 595-600, 2001.